

Measurements of small angle elastic \vec{p} -d scattering at 796 MeV using a recoil method

F. Irom,* G. J. Igo, J. B. McClelland,* and C. A. Whitten, Jr.
Department of Physics, University of California, Los Angeles, California 90024

M. Bleszynski
Department of Physics, University of California, Los Angeles, California 90024
and Los Alamos National Laboratory, Los Alamos, New Mexico 87545

(Received 26 April 1983)

The energy spectra of deuterons recoiling from a deuterium gas target bombarded by transversely polarized 796-MeV protons have been measured to obtain the differential cross sections, $d\sigma/dt$, and analyzing powers, $A_y(t)$, for \vec{p} -d elastic scattering over a range of laboratory angles from 4.53° to 13.02° , corresponding to a range of four-momentum transfer squared, $|t|$, from 0.013 to 0.108 GeV^2/c^2 . Employing several sets of nucleon-nucleon, N-N, amplitudes obtained from N-N phase shift analyses, comparisons are made between the experimental data and the predictions of a multiple scattering theory. In this region of four-momentum transfer, A_y is shown to depend almost entirely on the spin-independent and spin-orbit N-N amplitudes.

$$\left[\text{NULCEAR REACTIONS } d(\vec{p},p)d, E=796 \text{ MeV; measured } d\sigma/dt(\theta) \text{ and } A_y(\theta); \text{ comparison with multiple-scattering theory using free N-N amplitudes, } -t=0.013-0.108 \text{ GeV}^2/c^2, \Delta t=1.88 \times 10^{-3} \text{ GeV}^2/c^2. \right]$$

I. INTRODUCTION

The study of polarized proton-deuteron (\vec{p},d) elastic scattering at intermediate energies (~ 1 GeV) and small momentum transfers, q , is of considerable interest. Since the small binding energy of the deuteron produces a rather large average separation distance between its constituent proton and neutron, hadron-deuteron scattering can be particularly well described by multiple scattering theories which use free hadron-nucleon amplitudes. A formalism¹ has recently been developed which provides a complete description of hadron-deuteron elastic scattering at intermediate energies in terms of hadron-nucleon amplitudes and a deuteron wave function, using an approach analogous to Glauber theory. A very precise framework is provided by this formalism for studying the dependence of p-d elastic scattering observables on the p-n amplitude, an amplitude which is quite difficult to determine independently, particularly at small momentum transfers. This formalism has recently been used to analyze experimental data on vector and tensor analyzing powers for p-d elastic scattering at intermediate energies.^{2,3}

From a theoretical standpoint it is simpler and more transparent to extract information on the projectile-neutron amplitude at small q^2 from projectile-deuteron elastic scattering than from breakup processes. As is well known, for breakup processes corrections due to final state interactions play a major role at small q^2 , since the probability for reformation of the deuteron in the final state becomes large when the momentum transfer imparted to the target becomes small. However, 800 MeV quasifree p-p and p-n analyzing powers at small momentum transfers

have recently been obtained from 800 MeV proton scattering on deuterium.⁴ Agreement between free and quasifree p-p results indicates the validity of the extraction of free p-n amplitudes from quasifree processes.

The precise knowledge of p-p and p-n amplitudes at small momentum transfers ($q \lesssim 0.2$ GeV/c) is particularly important in intermediate energy nuclear structure studies which use data from proton-nucleus elastic and inelastic scattering. In the theoretical analyses of these data the small momentum transfer behavior of the elementary N-N amplitudes are most relevant since the contributions from large momentum transfers are suppressed due to the rapid falloff of the nuclear form factors as a function of q^2 .

In the present paper we report on the measurement of both the differential cross section, $d\sigma/dt$, and analyzing power, A_y , for 796 MeV \vec{p} -d elastic scattering over a range of four-momentum-transfer squared $-t$, $-t=q^2$, from 0.013 GeV^2/c^2 to 0.108 GeV^2/c^2 . These data have been compared with the predictions of hadron-deuteron elastic scattering formalism mentioned above. The sensitivity of these analyses to the various components of the N-N amplitudes, to the deuteron wave function, and to the double-scattering terms has been investigated.

II. THE EXPERIMENTAL METHOD

These \vec{p} -d elastic scattering measurements were made utilizing the External Proton Beam line (EPB) of the Los Alamos Meson Physics Facility (LAMPF). The experiment measured small angle elastic p-d scattering using a recoil technique. The experimental technique and setup have been discussed in some detail previously.^{5,6} In p-d

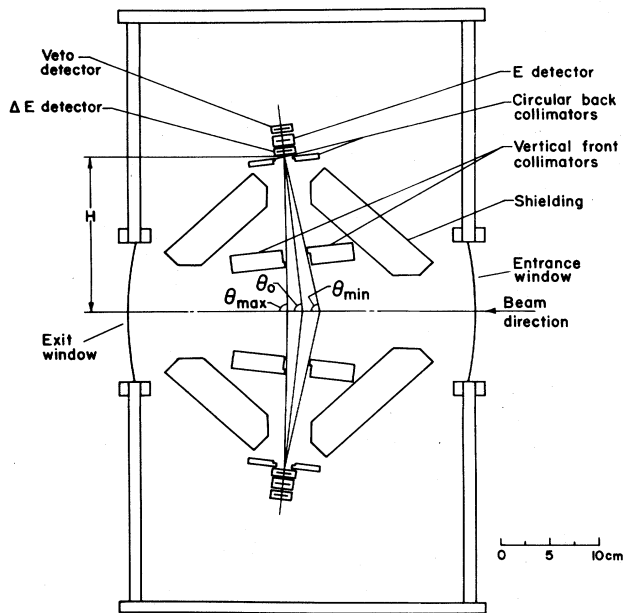


FIG. 1. The gas cell target box with the collimation systems and ΔE - E -VETO telescopes of solid state detectors.

elastic scattering the laboratory kinetic energy of the recoiling deuteron is a direct measure of the four-momentum transfer in the scattering process. Also, because the deuteron has no bound excited states, the only deuterons with laboratory scattering angles near 90° are from elastic scattering. In inelastic reactions involving pion production, the recoil deuteron is constrained kinematically to smaller angles ($\theta_{L_{\max}} = 61^\circ$ for $T_{pL} = 800$ MeV). Thus, we measured the deuteron energy spectra, dY/dT_d , through a suitable collimation system and extracted the angular distribution, $d\sigma/dt$, from these data.

The experimental setup, presented in Fig. 1, was a deuterium gas target viewed by a collimated detector system. The rear collimator, a circular aperture, has dimensions commensurate with the active areas of the detectors. Nearer the interaction region, vertical slits define an angular acceptance, θ_{\min} to θ_{\max} , for particle trajectories from the interaction region through the back slit. Recoil deuterons produced in the interaction region of the gas target are detected by two ΔE - E VETO telescopes of silicon surface barrier detectors mounted on movable arms on opposite sides of the beam. One arm consisted of a $50\text{-}\mu\text{m}$ ΔE detector, a $1400\text{-}\mu\text{m}$ E detector, and a $300\text{-}\mu\text{m}$ VETO detector; the other arm was of similar design but the ΔE detector was $100\text{-}\mu\text{m}$ thick. To obtain the energy spectra of recoil deuterons in the region above 20 MeV ($-t \gtrsim 0.073 \text{ GeV}^2/c^2$), the $1400\text{-}\mu\text{m}$ detectors were used as both ΔE and E detectors followed by a $300\text{-}\mu\text{m}$ VETO detector.

With the experimental setup displayed in Fig. 1, the differential cross section, $d\sigma/dt$, is related to the deuteron yield per kinetic energy interval, dY/dT_d , by⁵

$$\frac{d\sigma}{dt} = (dY/dT_d) [\pi/m_d] \frac{H \sin\theta_d}{nNA \cos(\theta_d - \theta_0)}. \quad (2.1)$$

Here A is the area of the circular back collimator, H is the perpendicular distance from the beam center line to the center of the back collimator, m_d is the mass of the deuteron, n is the number of deuterons per unit volume in the gas target, N is the flux of beam particles, and θ_0 is the angle between the center line of each telescope arm and the beam direction. The recoil angle, θ_d , may be calculated from the energy measurement.⁶

For data taken with the left (L) and right (R) ΔE - E -VETO telescopes ($T_d \lesssim 20$ MeV) the analyzing power, A_y , was calculated from the measured left-right asymmetry ϵ ,

$$\epsilon = A_y P_B = \frac{L - R}{L + R}, \quad (2.2)$$

where L and R represent geometrical means

$$L = [(dY/dT)_{R\uparrow} (dY/dT)_{L\downarrow}]^{1/2}, \quad (2.3a)$$

$$R = [(dY/dT)_{R\downarrow} (dY/dT)_{L\uparrow}]^{1/2}. \quad (2.3b)$$

P_B is the magnitude of the beam polarization normal to the scattering plane; and the arrows \uparrow (up) and \downarrow (down) represent the direction of the beam polarization. This technique cancels first order instrumental asymmetries. When only one telescope was used ($T_d \gtrsim 20$ MeV), A_y was calculated from

$$A_y = \frac{1}{P_B} \left[\frac{(dY'/dT)_{\downarrow} - (dY'/dT)_{\uparrow}}{(dY'/dT)_{\downarrow} + (dY'/dT)_{\uparrow}} \right]. \quad (2.4)$$

Here Y' denotes a yield normalized by the integrated beam intensity for a given direction of the beam polarization. As discussed in Ref. 6, the beam polarization P_B was measured by the EPB beam line polarimeter⁷ located downstream from our target gas cell.

Signals from the ΔE and E detectors were used to obtain particle identification signals⁸ and energy spectra. The energy scale for the detectors was calibrated using alpha sources. Our method requires the measurement of the energy spectra for recoil particles from elastic p-d scattering emanating from an interaction region defined by the cross sectional area of the beam and the collimation system. However, spurious events whose characteristics in the detector telescope mimic those of the recoil deuterons are superimposed on the real spectra. Sources of these background events could be the following: (1) reactions of the proton beam and halo with any material other than the target gas; (2) beam-target interactions not in the interaction region. This background spectrum was measured quite carefully⁶ in two types of background runs. In the first, the target cell was evacuated while all other conditions were kept the same as in a normal data run. In the second, the gas cell pressure was maintained, but the front slit was closed, thereby removing only the recoil particles produced in the interaction volume. To within the statistical accuracies of the measurements, the two types of background evaluation agreed. Also, the background measured by these two techniques was a small fraction of

TABLE I. p-d elastic cross section and analyzing power data at 796 MeV.

$\theta_{c.m.}$ (deg)	$-t$ (GeV/c) ²	$\frac{d\sigma}{dt}$ $\left[\frac{\text{mb}}{(\text{GeV}/c)^2} \right]$	A_y
7.97	0.0133	210.3±1.6	0.2735±0.0074
8.51	0.0152	193.6±1.5	0.2849±0.0076
9.02	0.0171	181.1±1.5	0.2927±0.0076
9.50	0.0189	171.9±1.3	0.3039±0.0057
9.97	0.0208	164.6±1.0	0.3151±0.0058
10.41	0.0227	158.3±1.0	0.3294±0.0060
10.83	0.0246	147.2±1.0	0.3271±0.0062
11.24	0.0265	139.2±0.9	0.3427±0.0063
11.63	0.0283	132.4±0.9	0.3527±0.0065
12.01	0.0302	123.9±0.9	0.3612±0.0067
12.38	0.0321	118.5±0.9	0.3668±0.0068
12.74	0.0340	112.8±0.8	0.3808±0.0070
13.08	0.0358	104.9±0.8	0.3844±0.0073
13.42	0.0377	101.3±0.8	0.3889±0.0074
13.76	0.0396	94.2±0.8	0.3863±0.0076
14.08	0.0415	89.3±0.7	0.3925±0.0078
14.40	0.0433	84.6±0.7	0.4069±0.0080
14.71	0.0452	80.7±0.7	0.4060±0.0082
15.01	0.0471	76.8±0.7	0.4068±0.0084
15.31	0.0490	73.1±0.7	0.4032±0.0086
15.60	0.0508	68.1±0.6	0.4134±0.0088
15.89	0.0527	66.5±0.6	0.4199±0.0090
16.17	0.0546	62.5±0.6	0.4153±0.0093
16.45	0.0565	59.3±0.6	0.4267±0.0095
16.72	0.0583	56.0±0.6	0.4177±0.0098
16.99	0.0602	53.9±0.6	0.414 ±0.010
17.25	0.0621	50.9±0.6	0.435 ±0.010
17.51	0.0640	48.6±0.5	0.438 ±0.010
17.77	0.0658	47.0±0.5	0.432 ±0.011
18.02	0.0677	44.5±0.5	0.447 ±0.011
18.27	0.0696	42.7±0.6	0.438 ±0.012
18.47	0.0711	41.1±0.7	0.435 ±0.014
18.81	0.0737	39.5±0.8	0.426 ±0.025
19.15	0.0763	37.6±0.8	0.432 ±0.025
19.48	0.0790	36.2±0.7	0.410 ±0.026
19.80	0.0816	34.1±0.7	0.426 ±0.027
20.12	0.0842	32.5±0.7	0.428 ±0.028
20.44	0.0868	31.2±0.7	0.421 ±0.028
20.75	0.0895	28.6±0.6	0.416 ±0.029
21.05	0.0921	27.7±0.6	0.421 ±0.029
21.35	0.0947	25.8±0.6	0.429 ±0.031
21.65	0.0974	24.6±0.6	0.401 ±0.031
21.94	0.1000	23.0±0.6	0.432 ±0.032
22.23	0.1026	21.9±0.6	0.455 ±0.033
22.52	0.1052	20.0±0.5	0.406 ±0.035
22.80	0.1079	19.3±0.5	0.393 ±0.035

the good events ($\leq 3\%$).

To obtain the deuteron energy spectra at the point of interaction, we corrected the experimental spectra for energy losses in the deuterium gas between the interaction volume and the telescope, and in the thin dead layers on the detector's surfaces.⁶ Energy straggling effects were much less than the bin size, 500 keV [$\Delta t = 1.88 \times 10^{-3}$ (GeV/c)²], in which the final data are presented.

Data were taken with an ~ 2 nA transversely polarized

(78%) proton beam and a deuterium pressure of 300 mm Hg. The pressure and temperature of the target gas were monitored to determine the gas density to better than $\pm 1\%$; and the incident beam flux was measured by a Faraday cup⁹ with an accuracy of $\pm 1-2\%$. We have determined the absolute normalization of the cross section data to an accuracy of $\pm 3\%$, while the statistical accuracy of the cross section data is always better than $\pm 2\%$. Table I presents the differential cross sections, $d\sigma/dt$, and

analyzing powers, A_y , obtained in this experiment as a function of $\theta_{c.m.}$ and $-t$. The errors listed, $\Delta d\sigma/dt$ and ΔA_y , include only contributions due to statistics and background subtraction. The larger errors in A_y for $-t \geq 0.073 \text{ GeV}^2/c^2$ reflect the shorter running periods used to obtain the recoil data with the $1400 \mu\text{m}$ – $1400 \mu\text{m}$ – $300 \mu\text{m}$ ΔE - E -VETO detector telescope.

$$\begin{aligned} \hat{F}_{pd} = & [(F_0^0 \sigma_0 + F_0^y \sigma_y) \hat{1}] + [(F_x^x \sigma_x) J_x + (F_y^0 \sigma_0 + F_y^y \sigma_y) J_y + (F_z^z \sigma_z) J_z] \\ & + [(F_{xx}^0 \sigma_0 + F_{xx}^y \sigma_y) Q_{xx} + (F_{yy}^0 \sigma_0 + F_{yy}^y \sigma_y) Q_{yy} + (F_{xy}^x \sigma_x) Q_{xy} + (F_{yz}^z \sigma_z) Q_{yz}] . \end{aligned} \quad (3.1)$$

Here the σ_i are spin- $\frac{1}{2}$ Pauli operators associated with the proton, and the J_i and Q_{ij} , $Q_{ij} = \frac{1}{2}(J_i J_j + J_j J_i) - \frac{2}{3} \delta_{ij} \hat{1}$, are spin-1 vector and quadrupole operators, respectively, associated with the deuteron. For a given subamplitude the superscript and the subscript denote the proton and deuteron operator, respectively. Formula (3.1) is given in a right-handed Cartesian frame of reference (x, y, z) where the x axis is parallel to $\vec{k}_i - \vec{k}_f$ and the z axis is parallel to $\vec{k}_i + \vec{k}_f$. General expressions can be obtained for A_y and $d\sigma/dt(I_0)$ in terms of these 12 amplitudes:

$$A_y = 12 \text{Re} [F_0^0 F_y^{0*} + \frac{2}{3} F_y^0 F_y^{y*} + \frac{2}{9} (F_{xx}^0 F_{xx}^{y*} + F_{yy}^0 F_{yy}^{y*}) - \frac{1}{9} (F_{xx}^0 F_{yy}^{y*} + F_{yy}^0 F_{xx}^{y*})] / I_0 , \quad (3.2)$$

$$\begin{aligned} I_0 = & 6 [|F_0^0|^2 + |F_y^0|^2 + \frac{2}{3} (|F_x^x|^2 + |F_y^0|^2 + |F_y^y|^2 + |F_z^z|^2) \\ & + \frac{2}{9} (|F_{xx}^0|^2 + |F_{yy}^0|^2 + |F_{xx}^y|^2 + |F_{yy}^y|^2) - \frac{2}{9} \text{Re} (F_{xx}^0 F_{yy}^{y*} + F_{yy}^0 F_{xx}^{y*}) + \frac{1}{6} |F_{xy}^x|^2 + \frac{1}{6} |F_{yz}^z|^2] . \end{aligned} \quad (3.3)$$

A prescription for the construction of all the amplitudes F_j^i and F_{jk}^i from the proton-proton (pp) and proton-neutron (pn) amplitudes is described in detail in Ref. 1. In general, each of these amplitudes is given as a sum of single and double scattering terms which depend upon all the spin components of the pp and np amplitudes and upon the S and D components of the deuteron wave function.

Figure 2 presents the A_y data measured in this experiment along with predictions obtained using the multiple scattering formalism discussed above and four recent sets of the pp and np amplitudes obtained by Arndt¹⁰ from phase shift analysis of N-N scattering data: SM82 (summer 1982), SP82 (spring 1982), WI81 (winter 1981), and C800. In these calculations we have used the parametrization of the deuteron wave function due to Reid.¹¹ It is seen

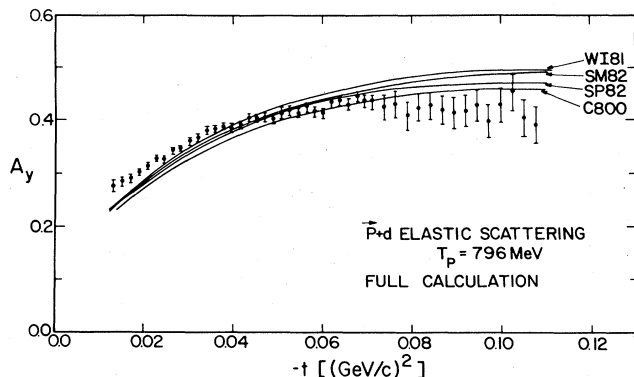


FIG. 2. A comparison of our A_y data for \bar{p} -d elastic scattering at 796 MeV with calculations based on the multiple scattering theory of Ref. 1 using as input the Arndt N-N amplitude sets SM82, SP82, WI81, and C800.

III. DISCUSSION

From parity conservation and the symmetry of the interaction under time reversal it follows¹ that 12 independent, complex amplitudes are necessary to completely describe p-d elastic scattering:

that there are significant differences between the four calculations and that all the calculations are lower than the experimental A_y data for $-t \leq 0.05 \text{ GeV}^2/c^2$ and higher than the experimental data for $-t \geq 0.08 \text{ GeV}^2/c^2$. Figure 3 presents the $d\sigma/dt$ data measured in this experiment along with calculations which use the four sets of N-N amplitudes. The differences in the predictions for $d\sigma/dt$ from the four sets of N-N amplitudes are negligible, but for $-t \geq 0.07 \text{ GeV}^2/c^2$ there is a significant difference between the experimental data and all four calculations.

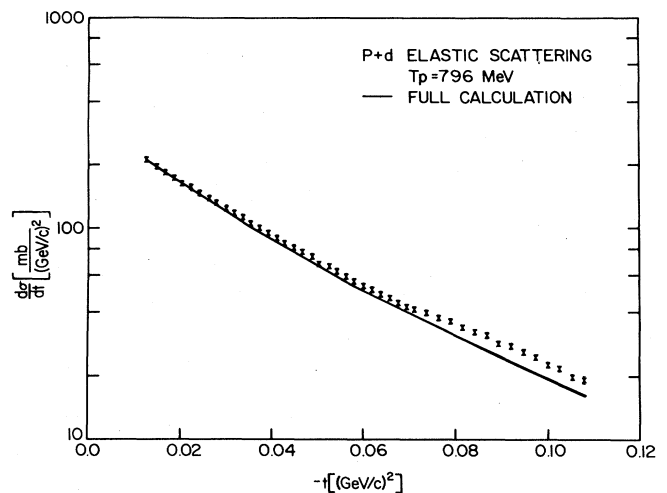


FIG. 3. A comparison of our $d\sigma/dt$ data for p-d elastic scattering at 796 MeV with calculations based on the multiple scattering theory of Ref. 1 using as input the Arndt N-N amplitude sets SM82, SP82, WI81, and C800. All four calculations are indistinguishable on the scale shown.

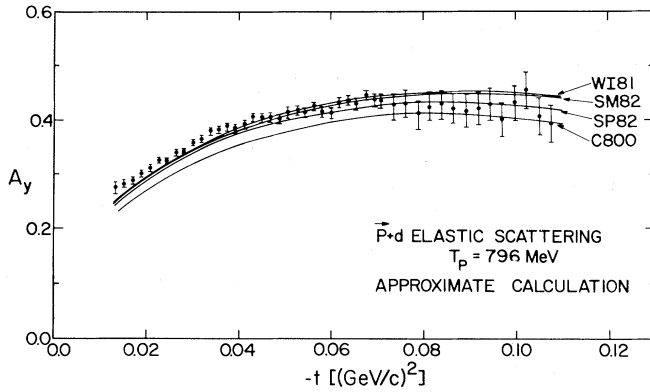


FIG. 4. Same as Fig. 2, but with calculations based on the approximate formula Eq. (3.5).

In order to better understand the origin of the differences between the calculations for A_y from the four sets of N-N amplitudes, we have numerically evaluated the strength of the various terms entering in Eq. (3.2). For values of $-t$ less than $0.1 \text{ GeV}^2/c^2$, A_y is given quite accurately by the expression

$$A_y \cong \frac{2 \operatorname{Re}(F_0^0 F_y^{0*})}{|F_0^0|^2 + |F_y^0|^2}. \quad (3.4)$$

Contributions from the other amplitudes in the complete expression [Eq. (3.2)] change the value for A_y given by Eq. (3.4) by less than 4%. Furthermore, the contributions from the double scattering terms, the spin-spin (double spin flip) terms in the N-N amplitude and from the D component of the deuteron wave function contribute at most a 5% effect in the approximate expression for A_y represented by Eq. (3.4) for $-t \lesssim 0.1 \text{ GeV}^2/c^2$. Thus, for $-t \lesssim 0.1 \text{ GeV}^2/c^2$, we have the following accurate approximation for A_y :

$$A_y \cong \frac{2 \operatorname{Re}(\bar{\alpha}^* i \bar{\gamma})}{|\bar{\alpha}|^2 + |\bar{\gamma}|^2}, \quad (3.5)$$

where $\bar{\alpha} = (\alpha_{pp} + \alpha_{pn})/2$ and $\bar{\gamma} = (\gamma_{pp} + \gamma_{pn})/2$ are the center-of-mass frame, isospin-averaged, spin-independent, and spin-orbit N-N amplitudes, respectively. Here the N-N amplitude is given by

$$M_{N-N} = \alpha + i\gamma(\vec{\sigma}_1 + \vec{\sigma}_2) \cdot \hat{n} + (\text{spin-spin terms}), \quad (3.6)$$

$$\hat{n} = \frac{\vec{k}_i \times \vec{k}_f}{|\vec{k}_i \times \vec{k}_f|}.$$

In Fig. 4 we present calculations of A_y based on Eq. (3.5) which use the same four sets of N-N amplitudes as the full [Eq. (3.2)] A_y calculations represented by Fig. 2. Inter and intra comparisons between the theoretical predictions represented by Figs. 2 and 4 lead one to conclude that Eq. (3.5) is a quite accurate approximate expression and that the difference between the various predictions for a given type of calculation come from the differences in the isospin averaged spin-independent and spin-orbit N-N

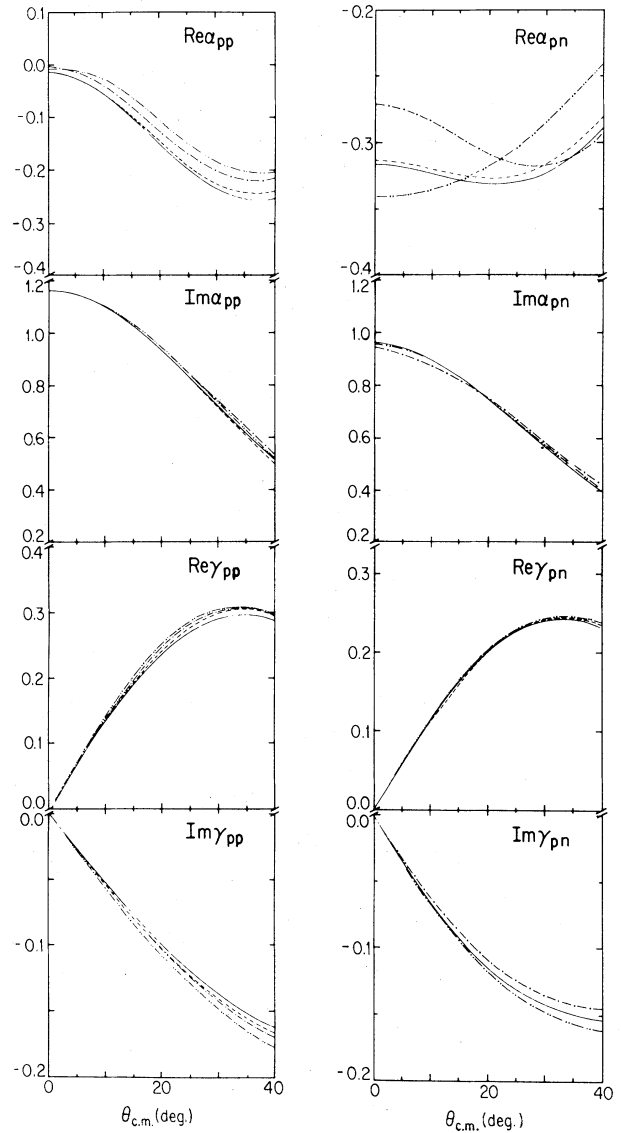


FIG. 5. Comparison of the N-N amplitudes α_{pp} , α_{pn} , γ_{pp} , and γ_{pn} from the four solution sets SM82 (---), SP82 (—), WI81 (---), and C800 (-.-).

amplitudes of the four solutions. Figure 5 presents the N-N amplitudes α_{pp} , α_{pn} , γ_{pp} , and γ_{pn} corresponding to the solutions C800, WI81, SP82, and SM82. The largest differences exist in the real parts of the spin-independent N-N amplitudes; and the analyzing power is very sensitive to the relative phase between α and γ . It would appear to be quite possible that N-N amplitudes somewhat different from the four sets used in the present analysis could both fit the currently available N-N data and provide closer agreement between our experimental A_y data and the predictions of a multiple scattering theory.

Although for $-t \lesssim 0.1 \text{ GeV}^2/c^2$, A_y is quite insensitive to contributions from the double scattering terms and the spin-spin components of the N-N amplitudes, this is not the case for $d\sigma/dt$. Figure 6 presents a full calculation

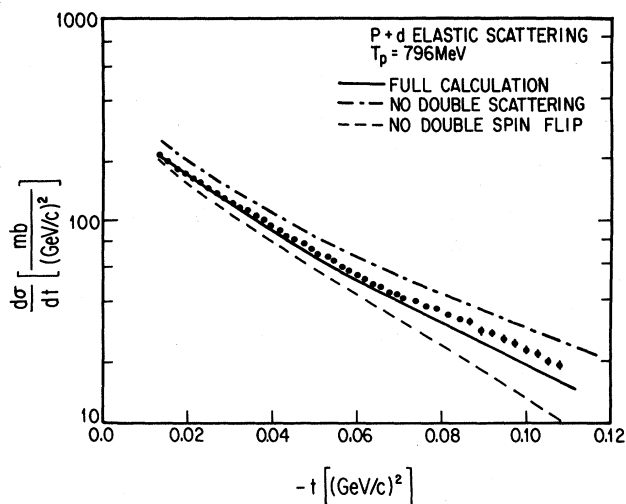


FIG. 6. A comparison of our $d\sigma/dt$ data for p - d elastic scattering at 796 MeV with a full multiple scattering calculation using the N-N amplitudes C800 and with calculations where either the double scattering terms or the double spin-flip N-N amplitudes were set equal to zero.

(essentially the same for all four sets of N-N amplitudes) along with calculations where either the double scattering terms or the spin-spin components of the N-N amplitudes were set to zero. Both contribute significantly to $d\sigma/dt$ down to very small $-t$.

To summarize, we have measured $d\sigma/dt$ and A_y for \bar{p} - d elastic scattering at 796 MeV in the range of four-momentum transfer squared from 0.013 to 0.108 GeV^2/c^2 . These data are compared with the predictions of a multiple scattering theory which uses free N-N amplitudes taken from the Arndt compilation. The discrepancies between theory and experiment for A_y can be possibly attributed to uncertainties in the N-N amplitudes, particularly the real part of the spin independent amplitudes.

ACKNOWLEDGMENTS

The assistance of O. Van Dyck and R. Werbeck of the LAMPF staff and H. Dajbkhsh during the data taking is greatly appreciated. This work was supported in part by the U.S. Department of Energy.

*Present address: Los Alamos National Laboratory, Los Alamos, NM 87545.

¹G. Alberi, M. Bleszynski, and T. Jaroszcwicz, *Ann. Phys. (N.Y.)* **192**, 233 (1982).

²M. Bleszynski *et al.*, *Phys. Lett.* **87B**, 198 (1979).

³M. Bleszynski *et al.*, *Phys. Lett.* **106B**, 42 (1981).

⁴M. L. Bartlett *et al.*, *Phys. Rev. C* **27**, 682 (1983).

⁵C. A. Whitten, Jr., *Nucl. Instrum. Methods* **128**, 93 (1975).

⁶F. Irom, G. J. Igo, J. B. McClelland, and C. A. Whitten, Jr.,

Phys. Rev. C **25**, 373 (1982).

⁷M. W. McNaughton, Los Alamos Scientific Laboratory Report No. LA-8307-MS, 1980.

⁸F. S. Goulding, D. A. Landis, J. Cerny, and H. L. Pehl, *Nucl. Instrum. Methods* **31**, 1 (1964).

⁹R. J. Barrett *et al.*, *Nucl. Instrum. Methods* **129**, 441 (1975).

¹⁰A. A. Arndt, *The Nucleon-Nucleon Computer Code* (Virginia Polytechnic Institute, Blacksburg, Virginia, 1980).

¹¹R. V. Reid, *Ann. Phys. (N.Y.)* **50**, 411 (1968).